

At4g29530 is a phosphoethanolamine phosphatase homologous to PECP1 with a role in flowering time regulation

Martin Tannert¹, Gerd Ulrich Balcke², Alain Tissier²  and Margret Köck^{1,*} 

¹Biocenter, Martin Luther University Halle-Wittenberg, Weinbergweg 22, Halle (Saale) 06120, Germany, and

²Department Cell and Metabolic Biology, Institute of Plant Biochemistry, Weinberg 3, Halle (Saale) 06120, Germany

Received 25 February 2021; accepted 28 May 2021; published online 7 June 2021.

*For correspondence (email margret.koeck@biozentrum.uni-halle.de).

SUMMARY

Phosphatidylcholine (PC) and phosphatidylethanolamine (PE) are the most abundant phospholipids in membranes. The biosynthesis of phospholipids occurs mainly via the Kennedy pathway. Recent studies have shown that through this pathway, choline (Cho) moieties are synthesized through the methylation of phosphoethanolamine (PEtn) to phosphocholine (PCho) by phospho-base *N*-methyltransferase. In *Arabidopsis thaliana*, the phosphoethanolamine/phosphocholine phosphatase1 (PECP1) is described as an enzyme that regulates the synthesis of PCho by decreasing the PEtn level during phosphate starvation to avoid the energy-consuming methylation step. By homology search, we identified a gene (*At4g29530*) encoding a putative PECP1 homolog from *Arabidopsis* with a currently unknown biological function *in planta*. We found that *At4g29530* is not induced by phosphate starvation, and is mainly expressed in leaves and flowers. The analysis of null mutants and overexpression lines revealed that PEtn, rather than PCho, is the substrate *in vivo*, as in PECP1. Hydrophilic interaction chromatography-coupled mass spectrometry analysis of head group metabolites shows an increased PEtn level and decreased ethanolamine level in null mutants. *At4g29530* null mutants have an early flowering phenotype, which is corroborated by a higher PC/PE ratio. Furthermore, we found an increased PCho level. The choline level was not changed, so the results corroborate that the PEtn-dependent pathway is the main route for the generation of Cho moieties. We assume that the PEtn-hydrolyzing enzyme participates in fine-tuning the metabolic pathway, and helps prevent the energy-consuming biosynthesis of PCho through the methylation pathway.

Keywords: *Arabidopsis thaliana*, choline, ethanolamine, ethanolamine kinase, hydrophilic interaction chromatography, phosphoethanolamine *N*-methyltransferase, phosphoethanolamine/phosphocholine phosphatase, phosphocholine, phosphoethanolamine, phospholipid.

INTRODUCTION

The glycerophospholipids phosphatidylcholine (PC) and phosphatidylethanolamine (PE) are the two most abundant phospholipid species in biological membranes of eukaryotic cells (Gibellini and Smith, 2010). Furthermore, such phospholipids function as signaling molecules and as substrates for the biosynthesis of storage lipids (Lin *et al.*, 2015). The *de novo* biosynthesis of PE and PC in most eukaryotic cells occurs through the Kennedy pathway (Figure 1; Gibellini and Smith, 2010; Kennedy and Weiss, 1956). The biosynthesis of the two phospholipids starts with ethanolamine (Etn) or choline (Cho; Kwon *et al.*, 2012). Choline/ethanolamine kinases (CEKs) produce phosphoethanolamine (PEtn) or phosphocholine (PCho) by the phosphorylation of Etn or Cho (Gibellini and Smith, 2010).

Afterwards, cytidine diphosphocholine (CDP)-activated Cho and CDP-activated Etn are synthesized by the CTP:phosphoethanolamine cytidyltransferase (PECT) and by the CTD:phosphorylcholine cytidyltransferases (CCT1/2), respectively. The syntheses of the intermediates CDP-Etn and CDP-Cho are regarded as rate-limiting steps in the Kennedy pathway (Inatsugi *et al.*, 2009; Mizoi *et al.*, 2006). In the next step, PE and PC are finally synthesized by an aminoalcoholphosphotransferase (AAPT; Alatorre-Cobos *et al.*, 2012; Yunus *et al.*, 2016). In plants, Etn is directly synthesized from serine by the unique enzyme serine decarboxylase (SDC; Mudd and Datko, 1989; Rontein *et al.*, 2003). The synthesis of choline moieties, however, requires three sequential *N*-methylation steps of Etn or PEtn. The PEtn-dependent pathway is described as the dominant

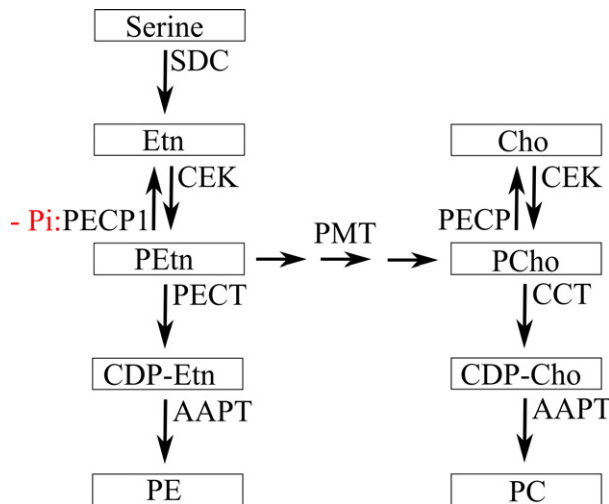


Figure 1. Synthesis and metabolism of ethanolamine (Etn) and choline (Cho) in Arabidopsis, including the two branches of the Kennedy pathway. Arrows indicate *de novo* biosynthesis of phospholipids PE and PC, respectively. Compounds are framed: Cho, choline; CDP-Cho, cytidine diphosphocholine; CDP-Etn, cytidine diphosphoethanolamine; Etn, ethanolamine; PCho, phosphocholine; PEtn, phosphoethanolamine; PC, phosphatidylcholine; PE, phosphatidylethanolamine. Enzyme names are placed on arrows: AAPT, aminoalcohol aminophosphotransferase; CEK, choline/ethanolamine kinase; CCT, CTP:phosphorylcholine cytidyltransferase; PMT, phospho-base *N*-methyltransferase; PECT, CTP:phosphorylethanolamine cytidyltransferase; PECP1, phosphoethanolamine/phosphocholine phosphatase1; SDC, serine decarboxylase.

methylation route, and is therefore essential for the entire pathway, especially for PC synthesis in plants (McNeil *et al.*, 2000). The reaction is catalyzed by the cytosolic enzyme phospho-base *N*-methyltransferase (PMT/PEAMT/NMT; Bolognese and McCraw, 2000). The *Arabidopsis thaliana* genome carries three gene loci encoding PMT/PEAMT/NMT proteins. All three PMTs catalyze methylation steps from PEtn to PCho. Accordingly, the substrate PEtn as the precursor of PCho and all derived Cho moieties has a significant influence on PC and PE biosynthesis, and on plant growth. In addition to CEKs, phosphatases (PECP) are known to catalyze the reverse reaction by hydrolyzing phosphorylated head groups (Figure 1).

Phosphoethanolamine/phosphocholine phosphatase1 from *A. thaliana* (PECP1; *At1g17710*), a member of the haloacid dehalogenase (HAD) superfamily, uses both PEtn and PCho as substrates *in vitro* (May *et al.*, 2012). Analyses of *pecp1* knockout mutants and overexpression lines have demonstrated that PECP1 uses only PEtn as substrate, and reduces the PEtn level under phosphate starvation (Tannert *et al.*, 2018). Further *in vitro* studies revealed that another phosphatase, PPsPase1/PS2/PECP2 (phosphate starvation gene 2; *At1g73010*), exhibited the highest substrate activity for pyrophosphate, but also showed activity for PEtn and PCho (May *et al.*, 2011). It is assumed that PPsPase1/PS2/PECP2 also functions as PEC-phosphatase and uses PEtn/PCho as substrates *in vivo*, because both phosphatases

belong to the same HAD-like phosphatase family and are co-expressed under phosphate starvation (Angkawijaya *et al.*, 2019; Hanchi *et al.*, 2018). Recently, a gene sequence homologous to PECP1 and PPsPase1/PS2/PECP2 was described. The enzyme was named ThMPase1 (encoded by *At4g29530*) because it was shown to possess an *in vitro* enzyme activity with the substrate thiamine monophosphate (Hasnain *et al.*, 2016). However, analyses of a knockout mutant could not determine reduced thiamine monophosphate phosphatase activity in comparison with the wild-type, so the *in vivo* function of the enzyme is still unknown.

Due to the sequence homology of ThMPase1 to PECP1 as well as PPsPase1/PS2/PECP2, we wondered whether ThMPase1 could have a biological role as PECP. In this study, we investigated the enzymatic and metabolic functions of Arabidopsis ThMPase1. To analyze the metabolic behavior, we used an established liquid chromatography–mass spectrometry method, which allows quantitative and simultaneous measurement of free and phosphorylated polar head groups. We found that *in vitro* the preferred substrate of ThMPase1 is PEtn. In line with our *in vivo* studies, we changed the name of the gene to PECP3 and use this name throughout the report. We show that PECP3 is not phosphate starvation-inducible. The analysis of Arabidopsis *pecp3* T-DNA insertion and ectopic overexpression lines revealed that PECP3 uses only PEtn as substrate *in vivo*. Interestingly, *pecp3* T-DNA insertion mutants exhibit an early flowering phenotype. Metabolic analysis revealed a significant change in the levels of free and phosphorylated head groups in shoots. We suggest that PECP3 is required for the regulation of the PCho biosynthesis through the methylation pathway.

RESULTS

Computational analysis and PECP3 activity

ThMPase1, hereon referred to as PECP3 in the context of this study, encodes a 245-amino acid protein with a relative molecular mass of 28 050. It is 34 and 50 amino acids shorter than the primary sequence of PECP1 and PPsPase1/PS2/PECP2, respectively, raising questions as to whether the characteristic structural features of the HAD superfamily are present. The sequence alignment demonstrates that PECP3 possesses the three unique motifs that are highly conserved in the sequence of the members of the HAD superfamily (Figure S1a,b). To investigate whether PECP3 can use PEtn and PCho as substrates, recombinant PECP3 protein was expressed in *Escherichia coli* and purified from the soluble fraction using a Ni²⁺-Sepharose-activated column (Figure S2). The phosphatase activity was tested by monitoring the release of free phosphate from a range of phosphorylated compounds as putative substrates, including thiamine

monophosphate (ThMP). We observed that PECP3 had by far the highest catalytic activity for PEtn (1379.2 nmol min⁻¹ mg⁻¹ protein), followed by ThMP (895.3 nmol min⁻¹ mg⁻¹ protein) and PCho (314.6 nmol min⁻¹ mg⁻¹ protein; Table S2).

Spatial PECP3 gene expression in dependence of phosphate supply

To study the regulation of PECP3 gene expression by Pi starvation, we grew seedlings on phosphate-replete medium for 14 days. Then we transferred the seedlings to a phosphate-free medium for 48 h, followed by a retransfer to phosphate-replete medium for up to 48 h. We used *AtPECP1* as a transcriptional control in quantitative reverse transcription-polymerase chain reaction (qRT-PCR). PECP1 was described as being highly upregulated by Pi starvation (Tannert et al., 2018). As expected, after incubation under phosphate starvation for 24 h, the expression for PECP1 was increased 9.4-fold, while the amount of transcript increased 88-fold after 48 h of phosphate deficiency. And in addition, the transcriptional response almost reached basal levels after subsequent incubation of plants under phosphate-replete conditions for 3 h (Figure 2a). In contrast, PECP3 showed no transcriptional changes after the transfer to low-phosphate medium (Figure 2a). In comparison to PECP1, PECP3 showed a low level of expression at all times.

To investigate the organ distribution of PECP3 expression, Arabidopsis plants were cultivated in a hydroponic system under phosphate-replete conditions. Organ samples were collected from 35-day-old adult plants and examined using qRT-PCR. We observed that PECP3 expression was highest in leaves and flowers (Figure 2b). Plants grown hydroponically under Pi deficiency conditions showed phosphate starvation symptoms, such as growth retardation, inhibition of primary roots and anthocyanin accumulation. Although the gene expression of PECP3 was significantly lower in 35-day-old plants under Pi starvation, we could not detect any difference between organs (Figure 2b). Because the transcript levels in 14-day-old seedlings of both phosphate-replete and phosphate-starved conditions were similar (Figure S3a), this result may indicate that the overall phosphate starvation response (PSR) downregulated PECP3 expression after long-term growth under phosphate starvation.

To investigate the promoter activity of PECP3, we used a histochemical GUS reporter assay. We fused the putative PECP3 promoter region with the β -glucuronidase (GUS) reporter gene. PromPECP3:GUS lines displayed a clear staining in leaf veins of 17-day-old plants [Figure 2c(a)]. Furthermore, the flower buds were strongly stained, especially the anthers [Figure 2c(b,c)]. The roots were not stained [Figure 2c(a)]. The difference between the GUS data and the transcript data for the root is possibly due to

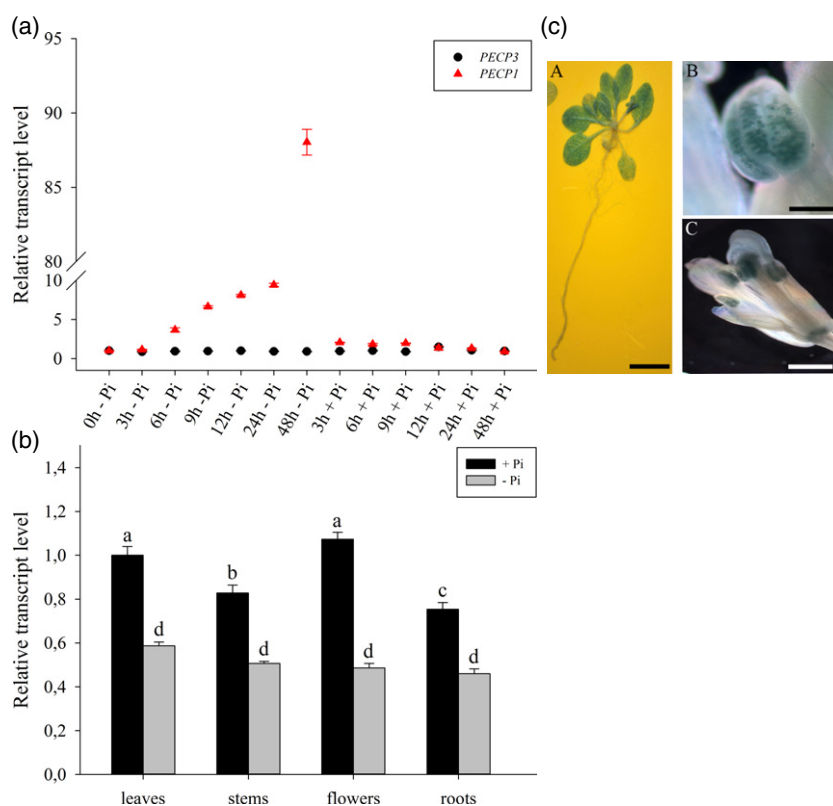


Figure 2. Analysis of PECP3 and PECP1 expression in changing Pi status.

(a) Plants were grown in liquid culture. *AtPECP1* (red triangle) and *PECP3* (black circle) transcript levels and those of the internal control *UBQ10* were determined by qRT-PCR. Transcripts were amplified over 30 cycles. Line -Phosphate: 14-day-old plants grown in full nutrition medium (sample 0 h/-Pi) were transferred to P-free medium for up to 48 h; after that, starved plants received 0.5 mM phosphate and grew for up to 48 h (Line +Phosphate); samples were taken as indicated. Expression levels are shown as the mean \pm SD from three biological replicates with three technical replicates for each.

(b) qRT-PCR analysis of *PECP3* expression in organs of 35-day-old plants cultivated hydroponically. Calibrator sample: leaves, normalized to *UBQ10*. Expression levels are shown as the mean \pm SD from four biological replicates with three technical replicates for each. One-way ANOVA was used; different letters indicate means that differ significantly ($P < 0.05$).

(c) PromPECP3:GUS expression in phosphate-replete plant line 4-3. Seventeen-day-old plant (a), anthers (b) and flower bud (c) of a 30-day-old plant. Scale bars: 10 mm (a); 20 μ m (b); 40 μ m (c). ANOVA, analysis of variance; PECP, phosphoethanolamine/phosphocholine phosphatase; qRT-PCR, quantitative reverse transcription-polymerase chain reaction; SD, standard deviation.

the lack of unknown regulatory elements in the promoter, which are located in more distant areas. However, the PromPECP3:GUS lines showed no changed expression pattern in shoots under Pi deficiency (Figure S3b).

In vivo enzyme activity and head group metabolite levels in knockout plants

To better understand the physiological functions of PECP3, we isolated the allelic T-DNA insertion lines *pecp3-1* and *pecp3-2* (Figure 3a). The T-DNA insertions in *pecp3-1/thmpase1-1* and in *pecp3-2/thmpase1-2* are located in the third intron (790 nucleotides downstream of the ATG codon) and in the second exon (307 nucleotides downstream of the ATG codon), respectively (Figure 3a). We selected homozygous plants for the respective T-DNA insertions and proved homozygosity by genotyping (Figure S4). The qRT-PCR analyses of the T-DNA insertion lines (primers were placed 3' of the insertions; Figure 3a) showed that the amounts were at the limit of detection (Figure 3b). In addition, semi-qRT-PCR could not detect any full-length transcript amount in *pecp3-1* or *pecp3-2* plants (Figure S5). Taken together, these results indicate that the *pecp3* lines are knockout mutants. *pecp3-1* and *pecp3-2* displayed no morphological growth phenotype (Figure S6).

Questions arose as to whether the knockout of the *PECP3* gene resulted in a higher expression of the *PECP1* or *PPsPase1/PS2/PECP2* gene to compensate the loss of PECP3 activity. We cultivated plants hydroponically, and samples were taken after 35 days. The qRT-PCR showed that the *PECP1* or *PPsPase1/PS2/PECP2* expression in the *pecp3* lines was neither increased in the leaves nor in the roots compared with the wild-type (Figure 3c).

Next, we examined whether the knockout lines *pecp3-1* and *pecp3-2* show reduced enzyme activity. To achieve this, we cultivated seedlings in liquid culture under phosphate-replete conditions for 9 days. We measured the enzyme activity by hydrolysis of PEtn and PCho in protein extracts of knockout mutant lines and wild-type plants (Figure 3d). The enzyme activity for the substrate PEtn was significantly reduced by 26.3% in the *pecp3-1* mutant line compared with Col-0. Using PCho as substrate, there was no difference between *pecp3-1* mutant line and the wild-type. The knockout mutant line *pecp3-2* showed the same behavior as *pecp3-1*. The enzyme activity was significantly reduced by 14.1% for the substrate PEtn.

To test the effect of missing PECP3 activity in *pecp3* mutant lines on metabolite levels, we analyzed the levels of head group metabolites in roots and shoots of phosphate-replete plants. The plants grew hydroponically, and samples were taken after 35 days. In shoots, the PEtn level was significantly increased by 27.1% in *pecp3-1* and 25.5% in *pecp3-2* knockout lines in comparison with the wild-type, while we did not find any difference in the PEtn

levels in the roots (Figure 4a). In roots of wild-type plants and the two mutant lines, Etn levels were similar, whereas the Etn levels of shoots were reduced by 33% in *pecp3-1* and by 21.9% in *pecp3-2* mutant line compared with the wild-type (Figure 4b). We could also determine a significantly greater amount of PCho in shoots of *pecp3* lines (Figure 4c), whereas the levels for Cho in the wild-type and *pecp3* mutant lines were almost equal (Figure 4d). We could not detect any difference in roots for either metabolite, PCho or Cho. The levels of ThMP and thiamine (Th) remained unchanged in roots and shoots of both mutants, *pecp3-1* and *pecp3-2/thmpase1-2*, when compared with the wild-type Col-0 (Figure 4e,f).

In addition, we cultivated plants of the mutant line *pecp3-1* under phosphate-starved conditions and examined metabolite levels. In comparison with wild-type shoot or root samples, the levels of all head group metabolites did not show any significant differences (Table S3). We also measured levels of PC and PE in WT and *pecp3* mutants, and found that the PC/PE ratio was significantly increased in *pecp3* mutants (Figure S8). Because PC plays a role in flowering, this prompted us to examine the flowering time phenotype of *pecp3* mutants.

***pecp3* plants display an early flowering phenotype**

We observed a different flowering behavior during the regular cultivation of the knockout lines. To study the flowering time in the *pecp3* plants, we cultivated the plants hydroponically and counted rosette leaves when the flower was 5 mm above the rosette. We found that the *pecp3* lines flowered earlier compared with the wild-type (Figure 5a). The flowering time was also analyzed in terms of days to flower. We found a significantly earlier flowering of both *pecp3-1* (1.6 days \pm 0.9) and *pecp3-2* (1.7 days \pm 0.9) compared with the Col-0 wild-type plants (Figure S9a).

In Arabidopsis, activation of FLOWERING LOCUS T (*FT*) transcription in leaf vascular tissue induces flowering. FT protein is exported to the phloem sieve elements from which it is transported to the shoot apex and triggers subsequent flower development (Corbesier *et al.*, 2007). We examined the expression of two FT-effector genes, namely APETALA1 (*AP1*) and SUPPRESSOR OF OVEREXPRESSION OF CONSTANS 1 (*SOC1*) in the apical meristem of *pecp3* plants and wild-type plants to test the initiation of flowering. The plants grew hydroponically, and samples for *AP1* were taken after 7, 17 and 19 days. The qRT-PCR analyses showed that the transcript amounts of *AP1* were increased threefold in the *pecp3-1* plants and 1.8-fold in the *pecp3-2* plants compared with the wild-type after 17 days (Figure 5b). After 19 days, in comparison with wild-type, the expression of *AP1* increased further, and was 6.2 and 4.6 times higher in *pecp3-1* and *pecp3-2* lines, respectively. The expression of *SOC1* was analyzed after 3 and 7 days,

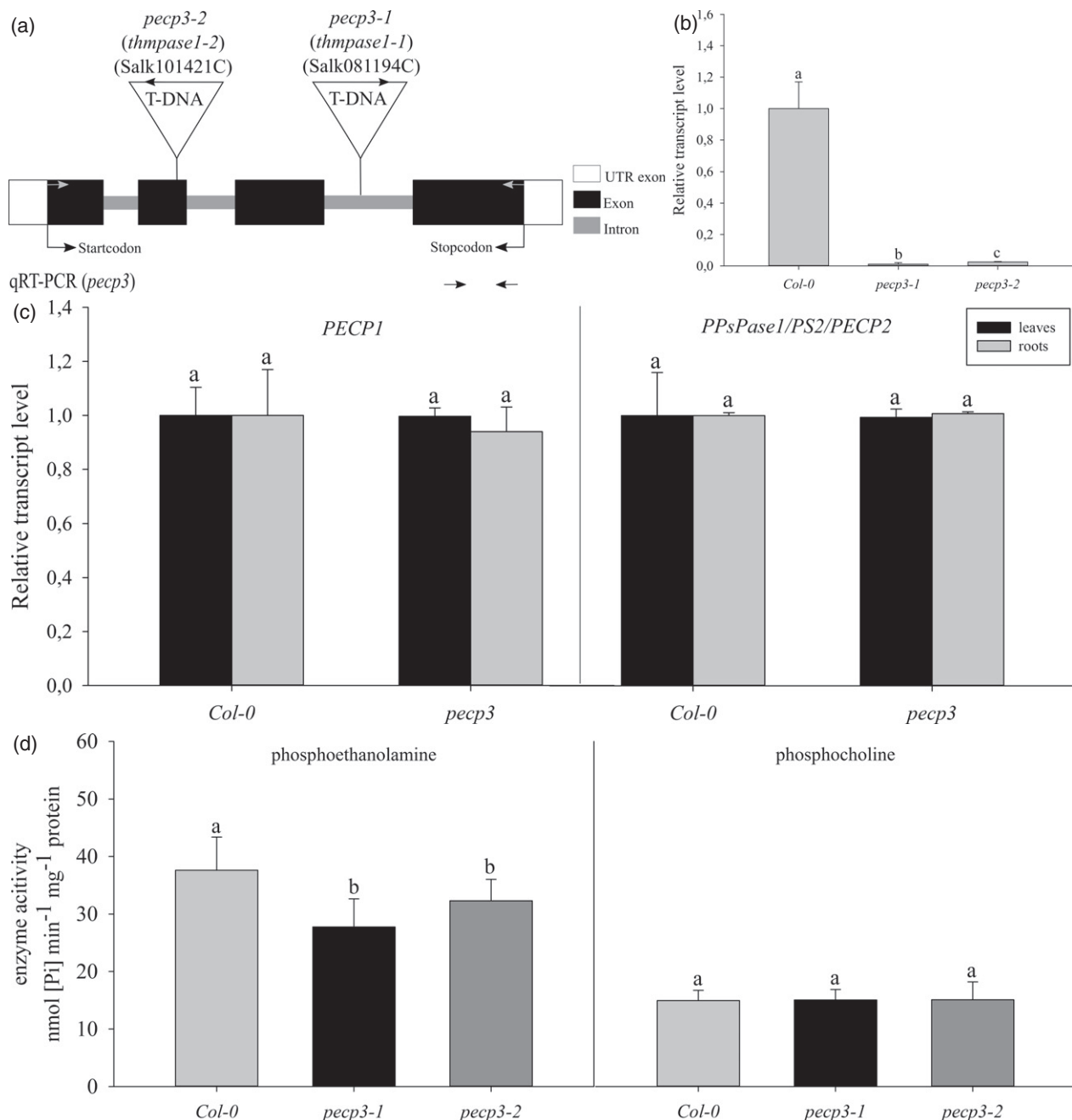


Figure 3. Molecular analysis of two independent Arabidopsis *PECP3* knockout mutant alleles.

(a) Positions of T-DNA insertion in the *PECP3* gene. Arrows mark the orientation of the T-DNA-derived primers (see Figure S4 for details of PCR genotyping and Table S1 for primers used). Gray arrows mark positions of primers used for sqRT-PCR (see Figure S5). Primer positions used for qRT-PCR are shown below the gene model (all arrows not on scale). The *pect3-1* and *pect3-2* T-DNA insertion lines are identical with the previously reported T-DNA mutants *thmpase1-1* (Hasnain *et al.*, 2016) and *thmpase1-2* (Hanchi *et al.*, 2018).

(b) RT-PCR analyses of *PECP3* expression under Pi-replete conditions revealed the presence of *pect3* null alleles. qRT-PCR with primers placed 3' of T-DNA insertions as shown in Figure 2(a). Calibrator sample: +Pi/Col-0, normalized to *UBQ10* ($n = 6$ biological replicates and three technical replicates). One-way ANOVA was used; different letters indicate means that differ significantly ($P < 0.05$).

(c) RT-PCR analyses of *PECP1* and *PPsPase1/PS2* expression under Pi-replete conditions in *pect3* plants revealed that *PECP1* and *PPsPase1/PS2* expression did not change compared with the wild-type (*Col-0*). Calibrator sample: +Pi/Col-0, leaves or roots; normalized to *UBQ10* ($n = 2$ biological replicates and two technical replicates). One-way ANOVA; different letters indicate means that differ significantly ($P < 0.05$).

(d) Measurement of *PECP3* enzyme activity with substrate PEtn or PCho, respectively, in the *pect3-1* (black) and *pect3-2* (dark gray) mutant lines compared with *Col-0* (gray). Samples were harvested from liquid-cultured seedlings grown in +Pi for 9 days. Two-way ANOVA was used to evaluate the differences between genotypes and treatments. The values are presented as means \pm SD ($n = 5$ –9 biological replicates and 3 technical replicates). Different letters indicate means that differ significantly ($P < 0.05$). ANOVA, analysis of variance; PCho, phosphocholine; PECP, phosphoethanolamine/phosphocholine phosphatase; PEtn, phosphoethanolamine; qRT-PCR, quantitative reverse transcription-polymerase chain reaction; SD, standard deviation.

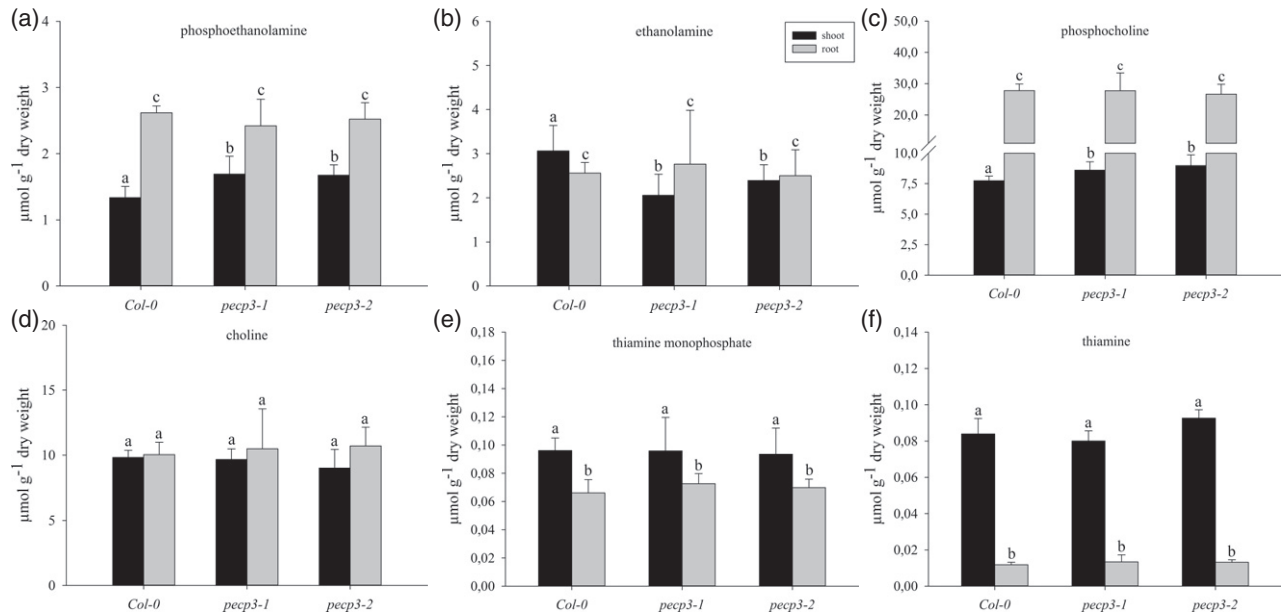


Figure 4. Loss of PECP3 activity change levels of the metabolites PEtn and Etn.

Content of head group metabolites in the shoots (black) or roots (gray) of *pectp3* knockout lines compared with the wild-type Col-0 as control determined using HILIC-MS/MS; (a) PEtn, (b) ethanolamine, (c) PCho, (d) choline, (e) ThMP, (f) Th. Samples were taken from plants grown hydroponically on +Pi medium (0.5 mM) under long-day conditions for 35 days. Two-way ANOVA was used to evaluate the differences between genotypes and treatments. The values shown represent the mean \pm SD ($n = 5$ biological replicates). Different letters indicate means that differ significantly ($P < 0.05$). ANOVA, analysis of variance; Etn, ethanolamine; HILIC-MS/MS, hydrophilic interaction chromatography-coupled mass spectrometry; PCho, phosphocholine; PECP, phosphoethanolamine/phosphocholine phosphatase; PEtn, phosphoethanolamine; SD, standard deviation; Th, thiamine; ThMP, thiamine monophosphate.

and revealed a 3.7-fold increase in *pectp3-1* and a 1.9-fold increase in *pectp3-2* mutant plants after 7 days when compared with wild-type plants (Figure S9b).

Analysis of constitutive ectopic expression lines of PECP3

Finally, to analyze the effects of phosphate-replete conditions on plant metabolism, we created overexpression lines (PromS35:*PECP3*). Based on qRT-PCR analyses, we selected two lines with greatly increased *PECP3* expression. The lines OE6 and OE10 produced 235- and 107-fold more *PECP3* transcripts, respectively, than Col-0 seedlings (Figure 6a). The overexpression plants displayed no morphological growth phenotype compared with the wild-type plants under phosphate-supplied or phosphate-starved conditions (Figure S6).

We examined whether the overexpression lines also showed a changed enzyme activity compared with the wild-type. We cultivated seedlings under phosphate-replete conditions for 9 days, and measured the enzyme activity by hydrolysis of PEtn and PCho in protein extracts of overexpression lines and wild-type plants (Figure 6b). We identified a significant increase of PEtn-hydrolyzing enzyme activity in both overexpression lines compared with the wild-type. The enzyme activity did not differ for PCho in wild-type and overexpression lines.

We also analyzed head group metabolites in roots and shoots of 35-day-old, hydroponically cultivated wild-type

and overexpression plants. We determined that the PEtn level in both shoots and roots was reduced by 62.9% and 67.1% in OE6, respectively, and by 54.4% and 61% in OE10, respectively, compared with Col-0 (Figure 7a). The Etn level, however, showed the greatest difference between overexpression lines and wild-type plants. Levels increased in shoots by 30.7-fold (OE6) and 33-fold (OE10), and in roots by fivefold (OE6) and 4.3-fold (OE10) (Figure 7b). In addition, the PCho level was reduced in the shoots by 36% (OE6) and 31.1% (OE10), and in the roots by 38.9% (OE6) and 34.3% (OE10) (Figure 7c). The level of Cho did not differ in roots and shoots for wild-type and overexpression lines (Figure 7d).

DISCUSSION

In this study, we investigated the enzymatic function *in vitro* and *in vivo* of PECP3/ThMPase1, and determined levels of headgroup metabolites of PE and PC. We were able to identify PECP3 as the isoenzyme of PECP1 and PPsase1/PS2/PECP2 and, in accordance with the InterPro predictive modeling software, as a member of the phosphatase PHOSPHO-type subfamily (Stewart *et al.*, 2003). Due to the fact that Hasnain *et al.* (2016) found the highest substrate preference of PECP3/ThMPase1 for ThMP and the artificial substrate *p*-nitrophenyl phosphate, we included both substrates in our tests. In contrast to a study by Hasnain *et al.* (2016), which did not analyze PEtn and PCho, we

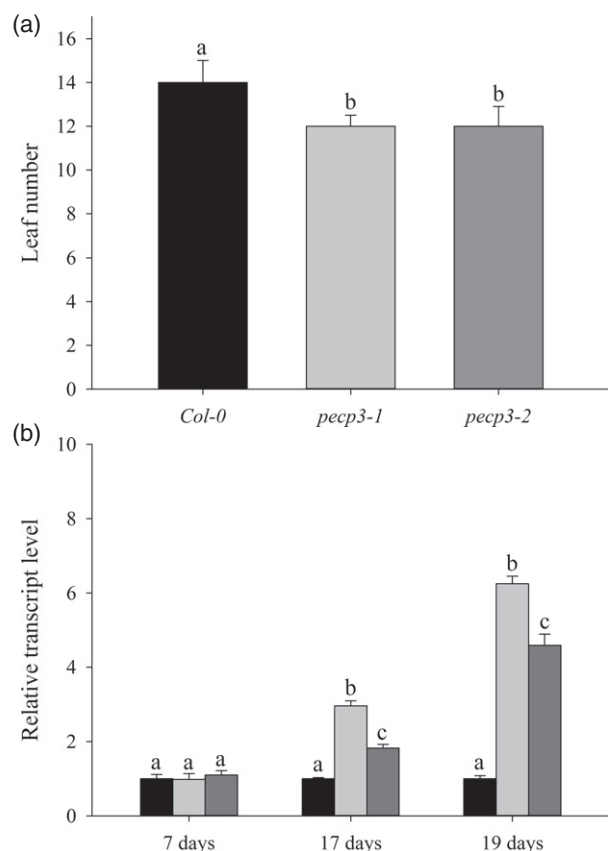


Figure 5. Effect of *pect3* knockout on flowering.

(a) Flowering time as measured by the number of leaves at flowering. The values are means \pm SD ($n = 30$ biological replicates). One-way ANOVA was used to analyze statistical difference. Different letters indicate means that differ significantly ($P < 0.05$).

(b) qRT-PCR analysis of *AP1* expression in shoot apex samples of 7-, 17- and 19-day-old plants of the *pect3* lines compared with the wild-type Col-0 grown in Pi-replete medium (calibrator Col-0, normalized to *UBQ10*). The values are means \pm SD ($n = 3$ biological replicates and 3 technical replicates). Two-way ANOVA was used to evaluate the differences between genotypes and developmental stages. Different letters indicate means that differ significantly ($P < 0.05$). ANOVA, analysis of variance; PECP3, phosphoethanolamine/phosphocholine phosphatase; qRT-PCR, quantitative reverse transcription-polymerase chain reaction; SD, standard deviation.

were able to compare the substrates PEtn, PCho and ThMP. PECP3 and PECP1 both have phosphatase activity with a higher substrate preference for PEtn than for PCho *in vitro* (May *et al.*, 2012); in addition, PECP3 prefers the substrate PEtn to ThMP.

Both *PECP1* and *PPsPase1/PS2/PECP2* are phosphate starvation-induced, and are mainly expressed in roots (Hanchi *et al.*, 2018; Tannert *et al.*, 2018). Expression studies have shown that *PECP1* is an important member of the PSR, and is highly co-expressed with PSR genes related to lipid metabolism (Angkawijaya and Nakamura, 2017; Lan *et al.*, 2015; Tannert *et al.*, 2018). In contrast to *PECP1*, our results show that *PECP3* is not phosphate starvation-

inducible (Figure 2a) and is expressed constitutively, showing higher expression in leaves and flowers than in stems and roots (Figure 2b,c). The investigation of *pect3* knockout mutants and the ectopic overexpression lines allowed us to answer our question of the enzymatic function of PECP3. Our results suggest that PECP3 does not act as a ThMP phosphatase *in vivo*. No difference in Th and ThMP levels was detected between *pect3-1/thmpase1-1* and *pect3-2/thmpase1-2* plants and the wild-type (Figure 4e,f). This result is in line with a study by Hasnain *et al.* (2016), showing that *thmpase1-1* mutant plants exhibited wild-type levels of Th vitamers [Th, ThMP, thiamine diphosphate (ThDP)]. Another line of evidence that PECP3/ThMPase1 does not contribute to the ThMP phosphatase activity comes from the double knockout mutant *thmpase1-1 th2-1*. The THIAMIN REQUIRING2 (TH2) gene product was found to be the main ThMP phosphatase in *A. thaliana* (Mimura *et al.*, 2016). Although the related gene (*At5g32470*) is deleted in the *th2-1* mutant, the ThDP synthesis is not completely eliminated; therefore, some ThMP phosphatase activity must be retained in *th2-1*. Double mutant individuals (*thmpase1-1 th2-1*) did not show more serious growth defects than *th2-1* single mutants (Mimura *et al.*, 2016), excluding an *in planta* function of PECP3/ThMPase1 as ThMP phosphatase.

In contrast, our results suggest that PECP3 is a PEtn-phosphatase. First, *pect3* plants have less PEtn-hydrolyzing enzyme activity than wild-type plants (Figure 3d), while the PCho hydrolysis activity was similar. This result shows strong similarities with a study of *pect1* null mutant lines by Tannert *et al.* (2018). Second, the corresponding overexpression lines showed an increased enzyme activity against the substrate PEtn, while the PCho hydrolysis was unaffected (Figure 6b). Third, shoots of both *pect3* lines had significantly greater PEtn levels but less Etn than the wild-type plants, which can be interpreted as the direct effect of the absence of PECP3 enzyme activity (Figure 4a,b). The result is consistent with *in vivo* enzyme analysis showing a PEtn-hydrolyzing activity for PECP3. Fourth, the ectopic overexpression of *PECP3* resulted in the accumulation of greater Etn amounts but smaller PEtn levels in the shoot of the lines OE6 and OE10 (Figure 7a,b), in accordance with the presence of additional PEtn phosphatase activity. When cultivated under phosphate-starved conditions, however, the *pect3-1* mutant did not show differences in metabolite levels (Table S3). We assume that the strong induction of *PECP1* and *PPsPase1/PS2/PECP2* activities upon phosphate starvation counteracts the increase in PEtn level in *pect3-1*.

The increased PEtn levels and the unchanged Etn levels in *pect3* lines do not give any indication of a changed Etn kinase activity catalyzing phosphorylation of Etn to PEtn, the biosynthetic forward reaction of the Kennedy pathway. In *A. thaliana*, four homologous CEKs were identified (Lin

Figure 6. Characterization of the ectopic overexpression lines (Prom35:*PECP3*).

(a) qRT-PCR analysis of *PECP3* expression in seedlings of the lines OE6 and OE10 compared with wild-type Col-0 plants grown in Pi-replete medium (calibrator Col-0; normalized to *UBQ10*). Values are means \pm SD ($n = 3$ biological replicates and 3 technical replicates). One-way ANOVA was used. Different letters indicate means that differ significantly ($P < 0.05$).

(b) Measurement of *PECP3* enzyme activity with substrate PEtn or PCho, respectively, in the ectopic overexpression lines of *PECP3*, OE6 (black) and OE10 (dark gray), compared with Col-0 (gray). Samples were harvested from liquid-cultured seedlings grown in +Pi for 9 days. The values are means \pm SD ($n = 5$ biological replicates and 3 technical replicates). One-way ANOVA was used to analyze differences. Different letters indicate means that differ significantly ($P < 0.05$). ANOVA, analysis of variance; PCho, phosphocholine; PECP, phosphoethanolamine/phosphocholine phosphatase; PEtn, phosphoethanolamine; qRT-PCR, quantitative reverse transcription-polymerase chain reaction; SD, standard deviation.

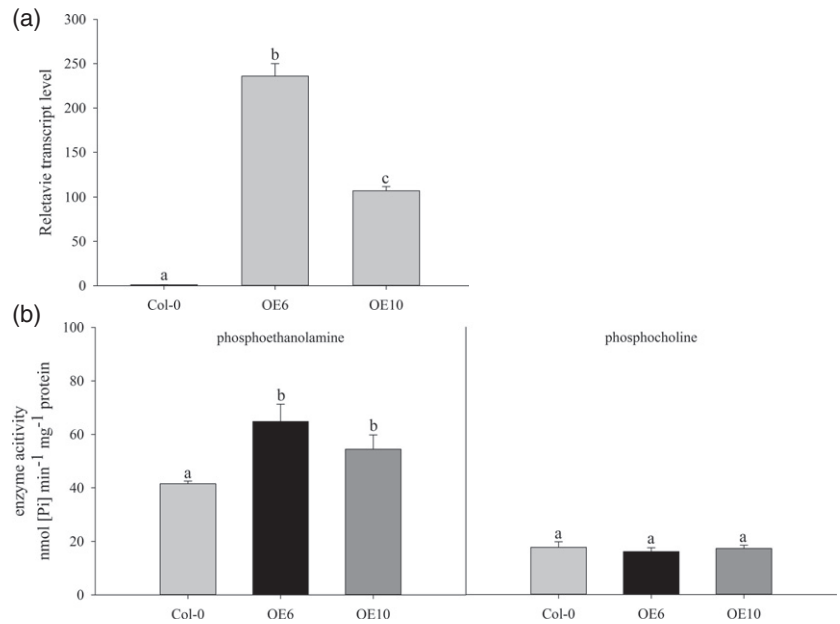
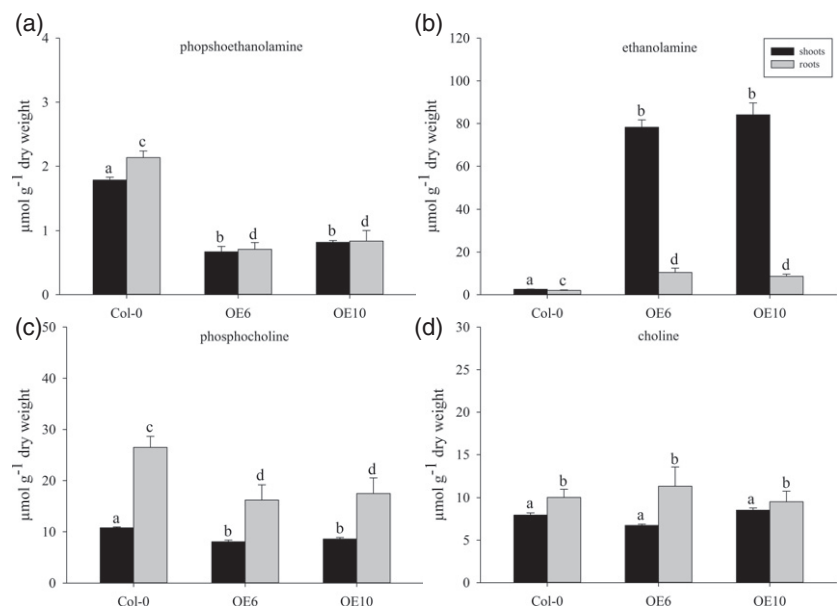


Figure 7. Enhanced *PECP3* activity reduces the PEtn amount. Levels of head group metabolites in the shoots (black bars) and the roots (gray bars) of overexpression lines OE6 and OE10 compared with wild-type Col-0 organs determined using HILIC-MS/MS; PEtn (a), ethanolamine (b), PCho (c), choline (d). Samples were taken from plants grown hydroponically on +Pi medium (0.5 mM) under long-day conditions (16 h photoperiod) for 35 days. Two-way ANOVA was used to evaluate the differences between organs and genotypes. Values represent the mean \pm SD ($n = 5$ biological replicates). Different letters indicate means that differ significantly ($P < 0.05$). ANOVA, analysis of variance; HILIC-MS/MS, hydrophilic interaction chromatography-coupled mass spectrometry; PCho, phosphocholine; PECP, phosphoethanolamine/phosphocholine phosphatase; PEtn, phosphoethanolamine; SD, standard deviation.



et al., 2015). Recent studies with T-DNA knockout lines and overexpression lines revealed that only CEK4 functions as an Etn kinase (Lin *et al.*, 2020). In contrast to PMT1, which is feedback inhibited by PCho (BeGora *et al.*, 2010), it is not known whether CEK4 is under metabolic control, for example, inhibited by its product, PEtn.

Phosphatidylcholine is a major phospholipid in plants, and has been demonstrated to play a critical role as structural component in cell membranes and in cellular signaling (Cruz-Ramirez *et al.*, 2004). Recent studies have confirmed that the methylation of PEtn is the sole entry point for *de novo* PC synthesis in Arabidopsis (Chen *et al.*,

2019). PCho is the precursor of PC and is converted to a phospholipid by CCT (Craddock *et al.*, 2015). The methylation is catalyzed by the enzyme PMT, which converts PEtn to PCho. As mentioned, there are three gene loci encoding PMT, PMT1 (*At3g18000*), PMT2 (*At1g48600*), and PMT3 (*At1g73600*), which are able to catalyze all three methylation steps from PEtn to PCho (Lee and Jez, 2017). In studies with ectopic overexpression lines of PMT, an increased PCho level could be found (McNeil *et al.*, 2001), whereas PMT knockout plants showed a reduced PCho level, up to a complete loss in the PMT triple knockout mutant (Liu *et al.*, 2019). Furthermore, it was found that PMT1 is

feedback-inhibited by PCho (BeGora *et al.*, 2010). Our qRT-PCR data revealed that the *pecp3* lines had a greater *PMT1* transcript amount than the wild-type (Figure S7). The increased transcript level of *PMT1* and the similar Cho levels (Figure 4d) in *pecp3* shoots compared with the wild-type allow the conclusion that the increased PCho amount (Figure 4c) in *pecp3* lines was caused by the PMT-mediated methylation of PEtn to PCho (Figure 8a). In contrast, the overexpression lines showed a reduced amount of PCho, probably caused by the decreased PEtn level at similar Cho levels, compared with the wild-type (Figure 6a, c,d). Our data are consistent with the recent finding that PCho biosynthesis is controlled by PMT/PEAMT/NMT activity (Chen *et al.*, 2019; Liu *et al.*, 2019). It has been reported that PMT shows the highest activity when plants grow in the light, and exhibits low to no activity after an extended dark period (Lorenzin *et al.*, 2001; Weretilnyk *et al.*, 1995). This light-dependent regulation could reduce the production of PCho in the dark when the continued synthesis of PCho is energetically disadvantageous to the plant (BeGora *et al.*, 2010). One possibility is that PECP3 degrades accumulated PEtn and deprives it from the methylation pathway to avoid the *de novo* production of PCho in the dark period. On the other hand, and although PECT is regarded as a rate-limiting step, the reduction of the PEtn level by PECP3 may impact PE biosynthesis as well.

The *pecp3* lines possess an increased PC:PE ratio compared with the wild-type, and were early flowering (Figures 5; Figures S8 and S9). Recent studies suggest that a connection exists between the activity of the FLOWERING LOCUS T (FT) protein, the systemic inducer of flowering,

and the phospholipid composition: (i) FT binds to PC *in vitro*, and *in vivo* PC levels are correlated with flowering time; (ii) an analysis of transgenic *amiPECT1* plants with reduced *PECT1* expression showed an increased PC:PE ratio compared with the wild-type and were early flowering (Nakamura *et al.*, 2014). FT forms with the transcription factor FD the florigen complex that promotes the transcriptional activation of *APETALA1* (*AP1*; Kawamoto *et al.*, 2015). The increased expression of *AP1* and *SOC1* in the *pecp3* knockout lines compared with the WT explains the observation of accelerated flowering (Figures 5b and S9b). Once the expression of *AP1* is initiated, this transcription factor orchestrates the floral transition by specifying floral meristem identity and regulating the expression of genes involved in flower development; *AP1* acts as a marker for the moment of the floral transition (Valentim *et al.*, 2015). Therefore, our results indicate that PECP3 has a function in flowering by regulating the biosynthesis of glycerolipid composition.

In conclusion, our results indicate that *PECP3* is a constitutively expressed gene, mostly in leaves and flowers. Taken together, the analysis of the T-DNA insertion lines and the overexpression lines suggest that the *PECP3* enzyme is a second PEtn-phosphatase alongside *PECP1* (Figure 8b). Considering our results, we decided it was appropriate to rename ThMPase1 to *PECP3*, following the suggestion of Hanchi *et al.* (2018) to rename PPsPase1/PS2 to *PECP2*. In accordance with several recent studies, we have also found that PEtn has an impact on the biosynthesis of PCho (Chen *et al.*, 2019; Cruz-Ramirez *et al.*, 2004; Liu *et al.*, 2018, 2019). Our data point to a regulatory role of

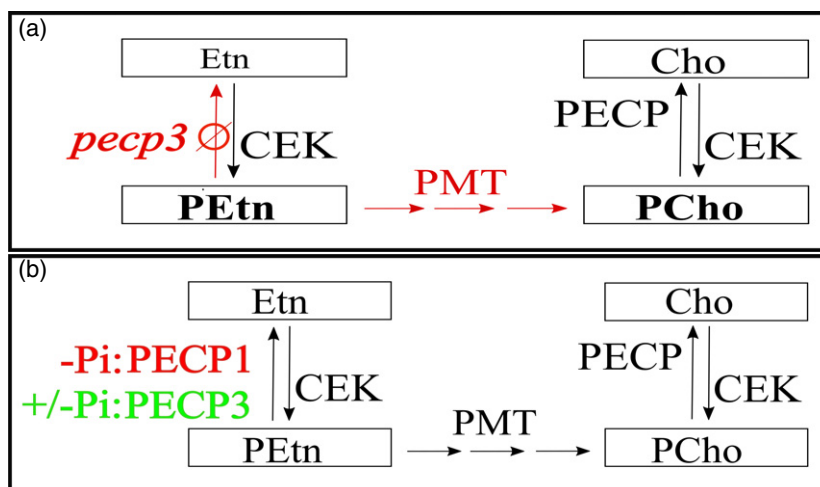


Figure 8. A model explaining the proposed function of the PECP3.

(a) A model of the metabolite flux affected by PECP3 knockout mutants (font sizes visualize relative metabolite levels, but are not to scale). During knockout of PECP3, PCho synthesis by PMT is upregulated because of the increased PEtn amount. The loss of PECP3 activity led to a decrease of the Etn level.

(b) A model for the role of PECP3 in the PEtn metabolism. We assume that PECP3 has a function in controlling the PEtn biosynthesis under still unknown metabolic conditions, thereby affecting the substrate availability for PMT, the enzyme generating Cho moieties. For PECP1, it was shown that the enzyme drastically reduces the PEtn level under phosphate starvation in order to avoid the energetically expensive methylation of PEtn by PMT (Tannert *et al.*, 2018). PECP, phosphoethanolamine/phosphocholine phosphatase; PEtn, phosphoethanolamine; PMT, phospho-base *N*-methyltransferase.

PECP3 in phospholipid metabolism under phosphate-replete conditions, with a particular impact on flowering time.

EXPERIMENTAL PROCEDURES

Plant material and growth conditions

Hydroponic culture, axenic liquid culture and agar plate cultivation were performed as described previously (Tannert *et al.*, 2018).

The cultivation system for the hydroponic cultivation of plants under sterile conditions consisted of stainless-steel wire mesh platforms with legs (125 μm mesh size) placed in commercially available glass jars, as described by Schlesier *et al.* (2003). Surface-sterilized seeds suspended in sterile agarose-sucrose solution (2% low melt agarose, 30% sucrose) were dispensed on the wire mesh platforms, and were grown on medium containing $\frac{1}{2}$ Murashige and Skoog medium (Duchefa Biochemie B.V., Haarlem, The Netherlands), 0.5% sucrose, 0.05% 2-(*N*-morpholino) ethanesulfonic acid (MES) at pH 5.8 for 14 days. Then the seedlings were transferred to null phosphate conditions ($\frac{1}{2}$ Murashige and Skoog medium without phosphate; Caisson Laboratories, North Logan, UT, USA; 0.625 mM KCl, 0.5% sucrose, 0.05% MES at pH 5.8) for 2 days. Subsequently, the plants were transferred back to the phosphate-replete medium for 2 days. Seedlings were cultivated in a growth chamber at 22°C with a 16 h photoperiod (50 $\mu\text{mol m}^{-2} \text{sec}^{-1}$).

Analysis of flowering time

For analysis of flowering time, plants were grown hydroponically in rooms with controlled environment under long days (16 h light/8 h dark). Flowering time was measured: (i) by counting the number of rosette leaves on the main stem; and (ii) by detecting the cultivation day on which the first flower of the inflorescence opened (days to flower). Thirty individuals for each genotype were used.

Characterization of T-DNA insertion lines

Seeds of two Arabidopsis T-DNA insertion lines (SALK_081194 and SALK_101421) were obtained from the European Arabidopsis Stock Centre (University of Nottingham). Genomic DNA was isolated from the leaves of about 4-week-old plants using standard procedures (Weigel and Glazebrook, 2002). PCR genotyping was performed using specific primers for the T-DNA left border and gene-specific primers corresponding to the regions flanking the respective T-DNA insertion (see Primer list in Table S1). The PCR products obtained were sequenced to confirm the location of the inserts. The knockout status of the T-DNA mutants was analyzed by RT-PCR methods using primers to amplify the coding region or primers placed downstream of the T-DNA insertions (Table S1).

Generation of PECP3 reporter lines for promoter activity

The putative PECP3 promoter sequence (690 bp upstream of translation start) was PCR-amplified using specific primers as stated in Table S1, and ligated into Entry Clone vector pENTR/D-TOPO according to manufacturer's instructions (Life Technologies, Carlsbad, CA, USA). To construct the vector for GUS expression of PECP3 promoter, a LR reaction was conducted with the construct pENTR/D-TOPO-Prom-PECP3 and vector pGWB3, containing a C-terminal GUS gene (Nakagawa *et al.*, 2007). The confirmed vector construct was transformed into *Agrobacterium tumefaciens* strain GV3101. *Arabidopsis thaliana* Col-0 plants were transformed using

standard procedures (Clough and Bent, 1998). After selection of transformed plants using kanamycin, the presence of the transgene was verified by PCR with primers amplifying the complete transgene. Homozygous PromPECP3:GUS lines were isolated.

Histochemistry of GUS staining

Harvested fresh tissues were immediately immersed in Fixing solution 1 [0.3% formaldehyde, 50 mM sodium phosphate, 500 mM ethylenediaminetetra-acetate (EDTA)] and then infiltrated under vacuum for 5 min. After 30 min incubation, the tissue was washed twice in the wash solution (50 mM sodium phosphate, 500 mM EDTA). The tissue was infiltrated with staining solution [0.5 mM X-Gluc (5-bromo-4-chloro-3-indolyl- β -D-glucuronide), 50 mM sodium phosphate, 500 mM EDTA, 0.5 mM potassium ferricyanide, 0.5 mM potassium ferrocyanide and 0.05% (w/v) Triton X-100] under vacuum for 5 min and incubated at 37°C overnight. The tissue was transferred in fixing solution 2 [45% (v/v) ethanol, 5% (v/v) formaldehyde and 5% (v/v) acetic acid] and incubated at 4°C for 2 h. For colored tissues, pigments were removed by immersing the tissue in 99% ethanol.

Generation of PECP3 overexpression lines

The open reading frame of PECP3 was amplified by PCR from cDNA and cloned with restriction-free cloning into pRT100 vector (Bond and Naus, 2012). According to Sharma *et al.* (2019), the cassette consisting of the CaMV 35S promoter, PECP3 ORF, and terminator sequence was cloned into pLSU4gg vector using Golden-Gate cloning. The confirmed vector construct was transformed into *A. tumefaciens* strain GV3101. *Arabidopsis thaliana* Col-0 plants were transformed using floral dip (Clough and Bent, 1998). After the selection of transformed plants using hygromycin, the presence of the transgene was verified by PCR. Homozygous Prom35S:PECP3 lines were isolated.

RNA extraction, cDNA synthesis and RT-PCR

RNA extraction and cDNA synthesis, RT- and qRT-PCR were performed as described previously (Tannert *et al.*, 2018). Primers are given in Table S1. Relative expression data were calculated using ubiquitin expression as the reference (*UBQ10*; *At4g05320*). Expression levels are given in relative quantity ($2^{-\Delta\Delta\text{Ct}}$). A CFX Connect system was used, and data evaluation was performed with the CFX Maestro software, version 4.1 (Bio-Rad Laboratories, Hercules, CA, USA).

Expression and purification of PECP3 protein

The open reading frame of PECP3 gene was cloned into pET28b(+) (Novagen, Darmstadt, Germany), adding the C-terminal sixfold His-tag encoded by the vector. A sequence-verified construct was introduced into *E. coli* BL21 (DE3). Bacteria were cultivated at 28°C in Luria-Bertani medium containing 100 $\mu\text{g ml}^{-1}$ ampicillin. At a cell density of $A_{600} = 0.7$, recombinant protein production was induced by treatment with 0.3 mM isopropyl β -D-1-thiogalactopyranoside. Cells were incubated for 4 h, and then harvested by centrifugation. The pellet was resuspended in binding buffer containing 10 mM TRIS/HCl pH 8, 350 mM NaCl, 20 mM imidazole and 0.2% IGEPAL, and the cells were lysed by sonication. The crude extract was cleared by centrifugation at 11 000 g and 4°C for 15 min. A Ni²⁺-Sepharose-activated column (20 ml; Fast Flow; GE Healthcare Bio-Sciences, Uppsala, Sweden) was equilibrated with 40 ml binding buffer. After washing with binding buffer, the column was eluted using a linear gradient of 0.02–0.8 M imidazole in binding buffer. Fractions containing enzyme activity were dialyzed three times for

1.5 h in 50 mM HEPES pH 7. Enzyme portions were stored on ice at 4°C for a maximum of 3 days.

Measurement of enzyme activity of PECP3

The *in vitro* assay (2.5 ml) contained 50 mM HEPES pH 6.5, 10 mM MgCl₂ and 5 mM substrate and enzyme (150 µl). The assay was started by adding enzyme, incubated for 30 min at 37°C. After several intervals, the reaction was stopped by mixing 0.5 ml of the assay mixture with 0.5 ml 20% trichloroacetic acid and centrifuging. Supernatants (1 ml) were collected and stored on ice.

For the *in vivo* assay, plant material was ground in liquid N₂. Samples (100 mg) were suspended in 300 µl extraction buffer (50 mM HEPES pH 7, 50 mM MgCl₂, 10 mM EDTA, 2 mM dithiothreitol, 10 µl ml⁻¹ Protease Inhibitor Cocktail for Plant Cell Extracts; Sigma/Merck KGaA, Darmstadt, Germany), vortexed and centrifuged, and supernatants were kept for further analyses. An enzyme activity assay (500 µl) containing 50 mM MES pH 6.5, 10 mM MgCl₂ and substrate (10 mM PEtn or PCho) was started by adding 25 µl supernatant and incubating for up to 18 min. After several intervals, the reaction was stopped by mixing 0.1 ml of the assay mixture with 0.1 ml 20% trichloroacetic acid and centrifuging. Supernatants (0.2 ml) were collected and stored on ice.

The supernatants of both assays were measured for phosphate by adding equal volumes of reagent I [40 mM (NH₄)₆Mo₇O₂₄, 2.5 N H₂SO₄] and reagent II [21 mM NH₄VO₃, 0.28 N HNO₃]. The absorption was measured at 405 nm. The amount of phosphate generated was calculated using a calibration curve. Protein concentration of the extract was determined by Bradford assay (Carl Roth, Karlsruhe, Germany).

Extraction and measurement of head group metabolites

Extraction and hydrophilic interaction chromatography coupled mass spectrometry were performed as described previously (Tannert *et al.*, 2018). The detection of metabolites was carried out by multiple reaction monitoring (Table S4).

Lipid extraction, separation, quantification and data analyses

Shoot samples (300 mg) homogenized under liquid nitrogen were analyzed by metaSysX GmbH using metaSysX standard procedures and in-house software (metaSysX GmbH, Potsdam, Germany). All lipids were grouped into their lipid classes, summed and normalized to 1/10 median of all lipid classes. Five biological replicates were analyzed.

Statistical analysis

Data sets were statistically analyzed by one-way or two-way analysis of variance followed by the Holm-Sidak *post hoc* test for testing differences between genotypes, organs and P treatments. Different letters were used to indicate significant difference ($P < 0.05$).

ACKNOWLEDGEMENTS

The authors would like to thank Franzisca Tannert (Martin Luther University Halle-Wittenberg) for assistance in cloning, and Hans-Peter Mock (Leibniz Institute of Plant Genetics and Crop Plant Research, Gatersleben, Germany) for providing devices for sterile hydroponic cultivation of plantlets. This work was supported by Martin Luther University Halle-Wittenberg, Halle (Saale), Germany. Open Access funding enabled and organized by Projekt DEAL.

AUTHOR CONTRIBUTIONS

MT and MK designed the research. MT performed the experiments, the statistical analysis, and the interpretation of the data with assistance from AT and MK. GUB provided chromatography and mass spectrometry expertise. MT and MK wrote the manuscript. AT executed critical revision of the article. MK was responsible for fund acquisition. All the authors read and discussed the manuscript, and give final approval of the version to be published.

CONFLICT OF INTEREST

The authors declare no competing financial interests.

DATA AVAILABILITY STATEMENT

All relevant data can be found within the manuscript and its supporting materials.

SUPPORTING INFORMATION

Additional Supporting Information may be found in the online version of this article.

Figure S1. Amino acid sequence analysis and phylogenetic relationship.

Figure S2. SDS-PAGE analysis of purified His-tagged PECP3 protein.

Figure S3. PECP3 expression in phosphate-deprived plants.

Figure S4. PCR genotyping of the T-DNA insertions in the PECP3 gene (At4g29530).

Figure S5. Analysis of PECP3 expression in *pecp3* lines.

Figure S6. Phenotypes of *pecp3* lines and Prom35S:PECP3 overexpression lines.

Figure S7. Analysis of PMT1 expression in *pecp3* lines.

Figure S8. PC:PE ratio in *pecp3* lines compared with wild-type plants.

Figure S9. Effect of *pecp3* knockout on flowering time and SOC expression.

Table S1. Sequences of primers used in this study

Table S2. Substrate specificity of recombinant PECP3

Table S3. Metabolite contents in P-deplete *pecp3-1* mutant plants

Table S4. MRM transitions for the metabolites analyzed by mass spectrometry

REFERENCES

- Alatorre-Cobos, F., Cruz-Ramirez, A., Hayden, C.A., Pérez-Torres, C.-A., Chauvin, A.-L., Ibarra-Laclette, E. *et al.* (2012) Translational regulation of *Arabidopsis* *XIPOTL1* is modulated by phosphocholine levels via the phylogenetically conserved upstream open reading frame 30. *Journal of Experimental Botany*, **63**(14), 5203–5221.
- Angkawijaya, A.E. & Nakamura, Y. (2017) *Arabidopsis* PECP1 and PS2 are phosphate starvation-inducible phosphocholine phosphatases. *Biochemical and Biophysical Research Communications*, **494**, 397–401.
- Angkawijaya, A.E., Ngo, A.H., Nguyen, V.C., Gunawan, F. & Nakamura, Y. (2019) Expression profiles of 2 phosphate starvation-inducible phosphocholine/phosphoethanolamine phosphatases, PECP1 and PS2, in *Arabidopsis*. *Frontiers in Plant Science*, **10**, 662. <https://doi.org/10.3389/fpls.2019.00662>.
- BeGora, M.D., Macleod, M.J., McCarry, B.E., Summers, P.S. & Weretilnyk, E.A. (2010) Identification of phosphomethylethanolamine *N*-

- methyltransferase from *Arabidopsis* and its role in choline and phospholipid metabolism. *Journal of Biological Chemistry*, **285**, 29147–29155.
- Bolognese, C.P. & McGraw, P.** (2000) The isolation and characterization in yeast of a gene for *Arabidopsis* S-adenosylmethionine:phosphoethanolamine-N-methyltransferase. *Plant Physiology*, **124**, 1800–1813.
- Bond, S. & Naus, C.C.** (2012) RF-Cloning.org: an online tool for the design of restriction-free cloning projects. *Nucleic Acids Research*, **40**, W209–W213.
- Chen, W., Taylor, M.C., Barrow, R.A., Croyal, M. & Masle, J.** (2019) Loss of phosphoethanolamine N-methyltransferases abolishes phosphatidylcholine synthesis and is lethal. *Plant Physiology*, **179**, 124–142.
- Clough, S.J. & Bent, A.F.** (1998) Floral dip: a simplified method for *Agrobacterium* mediated transformation of *Arabidopsis thaliana*. *The Plant Journal*, **16**(6), 735–743.
- Corbesier, L., Vincent, C., Jang, S., Fornara, F., Fan, Q., Searle, I. et al.** (2007) FT protein movement contributes to long-distance signaling in floral induction of *Arabidopsis*. *Science*, **316**(5827), 1030–1033.
- Craddock, C.P., Adams, N., Bryant, F.M., Kurup, S. & Eastmond, P.J.** (2015) Phosphatidic acid phosphohydrolase regulates phosphatidylcholine biosynthesis in *Arabidopsis* by phosphatidic acid-mediated activation of CTP:phosphocholine cytidyltransferase activity. *The Plant Cell*, **27**, 1251–1264.
- Cruz-Ramirez, A., Lopez-Bucio, J., Ramirez-Pimentel, G., Zurita-Silva, A., Sanchez-Calderon, L., Ramirez-Chavez, E. et al.** (2004) The *xipopt1* mutant of *Arabidopsis* reveals a critical role for phospholipid metabolism in root system development and epidermal cell integrity. *The Plant Cell*, **16**, 2020–2034.
- Gibellini, F. & Smith, T.K.** (2010) The Kennedy pathway – *de novo* synthesis of phosphatidylethanolamine and phosphatidylcholine. *IUBMB Life*, **62**, 414–428. <https://doi.org/10.1002/iub.337>
- Hanchi, M., Thibaud, M.-C., Legret, B., Kuwata, K., Pochon, N., Beisson, F. et al.** (2018) The phosphate fast-responsive genes *PECP1* and *PPsPase1* affect phosphocholine and phosphoethanolamine content. *Plant Physiology*, **176**, 2943–2962.
- Hasnain, G., Roje, S., Sa, N., Zallot, R., Ziemak, M.J., de Crecy-Lagard, V. et al.** (2016) Bacterial and plant HAD enzymes catalyses a missing phosphate step in thiamin diphosphate biosynthesis. *The Biochemical Journal*, **473**, 157–166.
- Inatsugi, R., Kawai, H., Yamaoka, Y., Yu, Y., Sekiguchi, A., Nakamura, M. et al.** (2009) Isoenzyme-specific modes of activation of CTP:phosphocholine cytidyltransferase in *Arabidopsis thaliana* at low temperature. *Plant and Cell Physiology*, **50**, 1727–1735.
- Kawamoto, N., Sasabe, M., Endo, M., Machida, Y. & Araki, T.** (2015) Calcium-dependent protein kinases responsible for the phosphorylation of a bZIP transcription factor FD crucial for the florigen complex formation. *Scientific Reports*, **5**(1), 8341. <https://doi.org/10.1038/srep08341>.
- Kennedy, E.P. & Weiss, S.B.** (1956) The function of cytidine coenzymes in the biosynthesis of phospholipids. *Journal of Biological Chemistry*, **222**, 193–214.
- Kwon, Y., Yu, S.-I., Lee, H., Yim, J.H., Zhu, J.-K. & Lee, B.-H.** (2012) *Arabidopsis* serine decarboxylase mutants implicate the roles of ethanolamine in plant growth and development. *International Journal of Molecular Sciences*, **13**, 3176–3188.
- Lan, P., Li, W. & Schmidt, W.** (2015) 'Omics' approaches towards understanding plant phosphorus acquisition and use. *Annual Review of Plant Biology*, **48**, 65–98.
- Lee, S.G. & Jez, J.M.** (2017) Conformational changes in the di-domain structure of *Arabidopsis* phosphoethanolamine methyltransferase leads to active-site formation. *Journal of Biological Chemistry*, **292**, 21690–21702.
- Lin, Y.-C., Araguirang, G.E., Ngo, A.H., Lin, K.T., Angkawijaya, A.E. & Nakamura, Y.** (2020) The four *Arabidopsis* choline/ethanolamine kinase isozymes play distinct roles in metabolism and development. *Plant Physiology*, **183**(1), 152–166.
- Lin, Y.-C., Liu, Y.-C. & Nakamura, Y.** (2015) The choline/ethanolamine kinase family in *Arabidopsis*: essential role of CEK4 in phospholipid biosynthesis and embryo development. *The Plant Cell*, **27**(5), 1497–1511.
- Liu, Y.-C., Lin, Y.-C., Kanehara, K. & Nakamura, Y.** (2018) A pair of phosphobase methyltransferases important for phosphatidylcholine biosynthesis in *Arabidopsis*. *The Plant Journal*, **96**, 1064–1075.
- Liu, Y.-C., Lin, Y.-C., Kanehara, K. & Nakamura, Y.** (2019) A methyltransferase trio essential for phosphatidylcholine biosynthesis and growth. *Plant Physiology*, **179**(2), 433–445.
- Lorenzin, D., Webb, C., Summers, P.S. & Weretilnyk, E.A.** (2001) Enzymes of choline synthesis in diverse plants: variation in phosphobase N-methyltransferase activities. *Canadian Journal of Botany*, **79**, 897–904.
- May, A., Berger, S., Hertel, T. & Köck, M.** (2011) The *Arabidopsis thaliana* phosphate starvation responsive gene *AtPPsPase1* encodes a novel type of inorganic pyrophosphatase. *Biochimica et Biophysica Acta*, **1810**, 178–185.
- May, A., Spinka, M. & Köck, M.** (2012) *Arabidopsis thaliana* PECP1 – enzymatic characterization and structural organization of the first plant phosphoethanolamine/phosphocholine phosphatase. *Biochimica et Biophysica Acta*, **1824**, 319–326.
- McNeil, S.D., Nuccio, M.L., Rhodes, D., Shachar-Hill, Y. & Hanson, A.D.** (2000) Radiotracer and computer modeling evidence that phospho-base methylation is the main route of choline synthesis in tobacco. *Plant Physiology*, **123**(1), 371–380.
- McNeil, S.D., Nuccio, M.L., Ziemak, M.J. & Hanson, A.D.** (2001) Enhanced synthesis of choline and glycine betaine in transgenic tobacco plants the overexpress phosphoethanolamine N-methyltransferase. *Proceedings of the National Academy of Sciences of the United States of America*, **98**, 10001–10005.
- Mimura, M., Zallot, R., Niehaus, T.D., Hasnain, G., Gidda, S.K., Nguyen, T.N.D. et al.** (2016) *Arabidopsis* TH2 encodes the orphan enzyme thiamin monophosphate phosphatase. *The Plant Cell*, **28**, 2683–2696.
- Mizoi, J., Nakamura, M. & Nishida, I.** (2006) Defects in CTP:phosphorylethanolamine cytidyltransferase affect embryonic and postembryonic development in *Arabidopsis*. *The Plant Cell*, **18**, 3370–4338.
- Mudd, S.H. & Datko, A.H.** (1989) Synthesis of ethanolamine and its regulation in *Lemna paucicostata*. *Plant Physiology*, **91**, 587–597.
- Nakagawa, T., Kurose, T., Hino, T., Tanaka, K., Kawamukai, M., Niwa, Y. et al.** (2007) Development of series of Gateway binary vectors, pGWBs, for realizing efficient construction of fusion genes for plant transformation. *Journal of Bioscience and Bioengineering*, **104**, 34–41.
- Nakamura, Y., Andres, F., Kanehara, K., Liu, Y.-C., Dörman, P. & Coupland, G.** (2014) *Arabidopsis* florigen FT binds to diurnally oscillating phospholipids that accelerate flowering. *Nature Communications*, **5**, 3553.
- Rontein, D., Rhodes, D. & Hanson, A.D.** (2003) Evidence from engineering that decarboxylation of free serine is the major source of ethanolamine moieties in plants. *Plant and Cell Physiology*, **44**(11), 1185–1191.
- Schlesier, B., Breton, F. & Mock, H.-P.** (2003) A hydroponic culture system for growing *Arabidopsis thaliana* plantlets under sterile conditions. *Plant Molecular Biology Reporter*, **21**, 449–456.
- Sharma, M., Kretschmer, C., Lampe, C., Stuttmann, J. & Klösgen, R.B.** (2019) Targeting specificity of nuclear-encoded organelle proteins with a self-assembling split-fluorescent protein toolkit. *Journal of Cell Science*, **132**(11), 230839. <https://doi.org/10.1242/jcs.230839>
- Stewart, A.J., Schmid, R., Blindauer, C.A., Paisey, S.J. & Farquharson, C.** (2003) Comparative modeling of human PHOSPHO1 reveals a new group of phosphatases within the haloacid dehalogenase superfamily. *Prot Engineering*, **16**, 889–895.
- Tannert, M., May, A., Diffe, D., Berger, S., Balcke, G.U., Tissier, A. et al.** (2018) Pi starvation-dependent regulation of ethanolamine metabolism by phosphoethanolamine phosphatase PECP1 in *Arabidopsis* roots. *Journal of Experimental Botany*, **69**, 467–481.
- Valentim, F.L., van Mourik, S., Pose, D., Kim, M.C., Schmid, M., van Ham, R.C.H.J. et al.** (2015) A quantitative and dynamic model of the *Arabidopsis* flowering time gene regulatory network. *PLoS One*, **10**(2), e0116973.
- Weigel, D. & Glazebrook, J.** (2002) *Arabidopsis: a laboratory manual*. New York, NY: Cold Spring Harbor Laboratory Press.
- Weretilnyk, E.A., Smith, D.D., Wilch, G.A. & Summers, P.S.** (1995) Enzymes of choline synthesis in spinach. Response of phospho-base N-methyltransferase activities to light and salinity. *Plant Physiology*, **109**(3), 1085–1091.
- Yunus, I.S., Liu, Y.-C. & Nakamura, Y.** (2016) The importance of serine decarboxylase1 (SDC1) and ethanolamine biosynthesis during embryogenesis of *Arabidopsis thaliana*. *The Plant Journal*, **88**, 559–569.